Theoretical Studies on the Low-Lying Electronic States of the HSO Neutral Radical and Its Cation

Bu-Tong Li, Zi-Zhang Wei, Hong-Xing Zhang,* and Chia-chung Sun

State Key Laboratory of Theoretical and Computational Chemistry, Institute of Theoretical Chemistry, Jilin University, Chang chun 130023, China

Received: May 16, 2006; In Final Form: July 19, 2006

Using the complete active space self-consistent field (CASSCF) method with large atomic natural orbital (ANO-L) basis set, four electronic states of the HSO neutral radical are optimized. The vertical transitions of the HSO neutral radical are investigated by using the same method under the basis set of ANO-L functions augmented with a series of adapted 1s1p1d Rydberg functions, through which eight valence states and eight Rydberg states are probed. Ionic states of the HSO neutral radical are extensively studied in both cases of the adiabatic and vertical ionization, from which the relatively complete understanding of ionization energies is given. To include further correlation effects, the second-order perturbation method (CASPT2) is implemented, and the comparison between CASSCF and CASPT2 methods is performed.

Introduction

HSO radical is an important molecule because it is the intermediate compound in the ozone-deleting cycle reactions:

$$HS + O_3 \rightarrow HSO + O_2 \quad (1)$$

$$HSO + O_3 \rightarrow HS + 2O_2 \quad (2-4)$$

Much experimental[1−12,32,34,41] and theoretical[13−31] research has been focused on the HSO molecule. However, most research is mainly about the enthalpy of formation of the HSO radical. Further information about the HSO radical, especially for the excited states and the ionization energies, is lacking. The first paper about the excited states of the HSO radical was published in 1977 by Schurath et al., in which a chemiluminescence spectrum above 5200 Å was assigned to $^2A'' \rightarrow {}^2A'$ character of the HSO neutral radical and the 0−0 band was also determined at 6960 Å in a $O/H_2S/O_3$ system.[1] In 1983, Kawasaki et al. measured the fluorescence lifetime of single vibration levels for $\tilde{A}^2A'$ under effusive flow conditions following excitation by a pulsed dye laser technology.[32] High-resolution laser-induced fluorescence (LIF) studies of the (003)−(000) band of the A−X transition for HSO and DSO also yielded the structural parameters in both states.[7,8] The fluorescence spectra and the fluorescent lifetimes of HSO ($\tilde{A}^2A'-X^2A''$) transition are measured in the wavelength range of 570−700 nm.[33] The vibrational excitation in the $v' = 2$ level of the v_3 mode is observed in the reaction: $HS + O_3 \rightarrow HSO^* + O_2$.[34] The ground state's molecular constants of the HSO radical have been obtained in several theoretical levels[13−31] and with several experimental technologies.[5,8] The HSO^+ cation can be expected to play an important role in the reactions relative to the reduced sulfur, and some geometry parameters and the harmonic frequencies values can be found for the ground and excited states of the HSO^+ cation,[31,41] and the ionization energy (9.918 ± 0.16 eV) was found in the spectral range (107−130 nm).[41] Apparently, the information about the excited states of these two molecules is still not enough.

So, in this paper, we reinvestigate the valence excited states of the HSO neutral radical and expand the research to a few Rydberg excited states by using complete active space self-consistent field (CASSCF) and second-order perturbation (CASPT2) methods. Furthermore, a few ionic states are probed, and the ionization energies are obtained adiabatically and vertically at the same theoretical level.

Calculation Method

The equilibrium geometries and vibration frequencies of the HSO species (neutral radical and cation) are determined in the CASSCF[35] method with the large atomic natural orbital (ANO-L)[36] basis set. To include more dynamic correlation energies, the multistate complete active space second-order perturbation (MS-CASPT2)[37,38] calculation is performed. All of the CASPT2 calculations in this paper are performed at the MS-CASPT2 level. With this multidimensional perturbative approach, we mix up a number of roots of the same symmetry provided by a previous state-average CASSCF calculation and produce the CASPT2 state. The coupling of a number of CASPT2 states and the nondiagonal elements of the Fock matrix are also considered in our CASPT2 calculations.

On the basis of the ground equilibrium geometry of the HSO neutral radical, the vertical transition calculations are carried out at CASSCF and CASPT2 levels by using the ANO-L^+ basis set, which is the ANO-L basis set augmented with a set of Rydberg orbital 1s1p1d. The universal exponents were optimized by Kaufmann et al. specially for Rydberg wave functions.[39] The ionization energies are also probed adiabatically and vertically by using the ANO-L basis set at both theoretical levels. We adopt the C_s symmetry in all of the calculations. The oscillator strengths values are obtained from the formula $f = 2/3(TDM)^2\Delta E$, in which ΔE is the perturbed CASPT2 energies and $TDM^2 = TDM_x^2 + TDM_y^2 + TDM_z^2$.

Choice of the active space is the most essential step in precise quantum calculations with the CASSCF method. In probe SCF,

* To whom correspondence should be addressed. E-mail: zhanghx@mail.jlu.edu.cn.

10.1021/jp063003s CCC: $33.50
Published on Web 08/23/2006

TABLE 1: Geometries of the States Optimized with CASSCF Method, the Relative Energies Calculated at CASPT2/CASSCF Level in ANO-L Basis Sets, and the Available Data from the Literature

	our calculated data					experimental and previous theoretical data			
state	CASSCF	CASPT2	R_{O-S}	Φ_{H-S-O}	R_{H-S}	energy	R_{O-S}	Φ_{H-S-O}	R_{H-S}
X^2A''	0.00	0.00	1.493	104.8	1.385		1.577[b]	101.30[b]	1.367[b]
							1.496[c]	104.70[c]	1.369[c]
							1.557[d]	101.3[d]	1.364
							1.540[e]	102.00[e]	1.350[e]
							1.389[f]	106.6[f]	1.494[f]
							1.571[h]	103.40[h]	1.361[h]
							1.528[h]	104.69[h]	1.355[h]
							1.519[h]	104.86[h]	1.354[h]
							1.518[h]	104.75[h]	1.363[h]
							1.506[h]	104.95[h]	1.361[h]
$1^2A'$	1.95	1.84	1.660	93.0	1.354		1.661[f]	95.7[f]	1.342[f]
						1.81[g]			
						1.81[h]	1.69−1.71[h]	90−97[h]	1.34[h]
						1.48[h]			
						1.71[h]			
							1.704[i]	95.00[i]	1.339[i]
$2^2A'$	4.07	3.92	1.538	107.8	1.676				
$3^2A''$	4.23	3.98	1.797	100.4	1.361				

[a] The energies are in units of eV, the bond lengths are in units of Å, and the bond angles are in unit of degree. The relative energies are obtained and compared to the ground energy −473.16187 au at the CASSCF level and −473.62117 au of the neutral radical at the CASPT2 level, respectively. [b] Ref 17. [c] Ref 29. [d] Ref 15. [e] Ref 5. [f] Ref 8. [g] Ref 32. [h] Ref 20. [i] Ref 14.

TABLE 2: Configuration Obtained Adiabatically at the CASPT2 Level by Using the ANO-L Basis Set

		configuration								
state	coeff	6a′	7a′	8a′	9a′	2a″	10a′	3a″	11a′	12a′
X^2A''	0.95	2	2	2	2	2	2	1	0	0
$1^2A'$	0.96	2	2	2	2	2	1	2	0	0
$2^2A'$	−0.89	2	2	2	2	2	2	0	1	0
	0.18	2	2	2	2	0	2	2	1	0
	0.23	2	2	2	2	2	1	2	0	0
$3^2A''$	−0.91	2	2	2	2	1	2	2	0	0
	−0.25	2	2	2	2	2	1	1	0	1
	0.10	2	2	2	2	1	0	2	0	0

calculation of the electronic configuration of the neutral ground radical is confirmed as (core)$(1a'')^2(6a')^2(7a')^2$ $(8a')^2(9a')^2(2a'')^2$-$(10a')^2(3a'')^1$. So, in the optimization process for the HSO radical, we choose 13 electrons activated in full valence space (10, 3), which means 10 a′ orbitals and three a″ orbitals. To keep a balance between the computation cost and the computation precise, we choose different active spaces for different vertical transition calculations, that is, 12 electrons activated in (10, 3) space for the vertical ionization process, five electrons activated in (2, 12) space in the vertical transition calculations of the HSO radical for the $^2A''$ symmetry, and seven electrons activated in (12, 3) space in the vertical transition calculations of the HSO radical for the $^2A'$ symmetry. All of the calculations are performed with the MOLCAS 5.4 quantum chemistry software[40] on SGI/O3800 servers.

Results and Discussion

Equilibrium Geometries of the HSO Neutral Radical. According to the energies listed in Table 1, the lowest state $1^2A''$ is confirmed as the ground state of the HSO neutral radical at both CASSCF and CASPT2 levels. As shown in Table 2, this state has a dominant leading configuration (core)$(6a')^2(7a')^2$ $(8a')^2(9a')^2(2a'')^2(10a')^2(3a'')^1$ with a coefficient of about 0.96. This assignment is in conflict with the multiconfiguration result at the CASSCF level by using the GAMESS package[20] but agrees with the CI results from ref 13. We have repeated the calculation in the same active space from ref 20, but the results are similar with this paper. Then, we can confirm that the configurations' difference is from the difference between the GAMESS and the MOLCAS softwares. Furthermore, it is surprising for the ground state that the single transition 2a″ → 3a″ has a coefficient value of −0.526.[20] From the plots of the electronic density shown in Figure 1, we can find that the single occupied 3a″ orbital is of π type antibonding character comprised essentially of the $3p_z$ of the sulfur atom and the $2p_z$ of the oxygen atom. The geometrical parameters of the ground state calculated by us are $R_{(O-S)} = 1.493$ Å, $R_{(H-S)} = 1.385$ Å, and $\Phi_{(H-S-O)} = 104.8°$, respectively, in excellent agreement with the experimental results $R_{(O-S)} = 1.494$ Å, $R_{(H-S)} = 1.389$ Å, and $\Phi_{(H-S-O)} = 106.6°$ from Doppler-limited dye laser excitation spectroscopy,[8] $R_{(O-S)} = 1.540$ Å, $R_{(H-S)} = 1.350$ Å, and $\Phi_{(H-S-O)} = 102.0°$ elucidated from the chemiluminescence spectrum from a $O/H_2S/O_3$ system,[5] and other available theoretical data listed in Table 1.[15,17,20,29]

The first excited state $1^2A'$ has a dominant leading configuration (core)$(6a')^2(7a')^2(8a')^2(9a')^2(2a'')^2(10a')^1(3a'')^2$ with a coefficient of about 0.96, which can be simply described by a single-electron transition 10a′ → 3a″. The 10a′ orbital is mainly of antibonding character coming from the interaction between the $3p_{xy}$ hybridized orbital of the sulfur atom and the $2p_{xy}$ hybridized orbital of the oxygen atom. A slight antibonding interaction between the hydrogen atom and the oxygen atom also exists in this orbital shown from the component analyses of the orbital. The 3a″ orbital is of antibonding character, resulting from the interaction between the $3p_z$ of the sulfur atom and the $2p_z$ of the oxygen atom as mentioned above and stands out off of the symmetrical plane. For the single-electon transition 10a′ → 3a″, the electron is promoted from an antibonding orbital to a stronger antibonding orbital and the bonding interaction between the hydrogen and the oxygen atoms is badly impaired. So, the $R_{(O-S)}$ is elongated to 0.167 Å, the $R_{(H-S)}$ is shortened to 0.031Å, and the $\Phi_{(H-S-O)}$ is reduced to 11.8° as compared to the ground state. For this state, the geometrical parameters are 1.660 Å, 1.354 Å, and 93.0° corresponding to $R_{(O-S)}$, $R_{(H-S)}$, and $\Phi_{(H-S-O)}$, respectively, which are consistent with the experimental data $R_{(O-S)} = 1.661$ Å, $R_{(H-S)} = 1.342$ Å, and $\Phi_{(H-S-O)} = 95.7°$ determined by the Doppler-limited dye laser excitation spectroscopy technology and better than theoretically

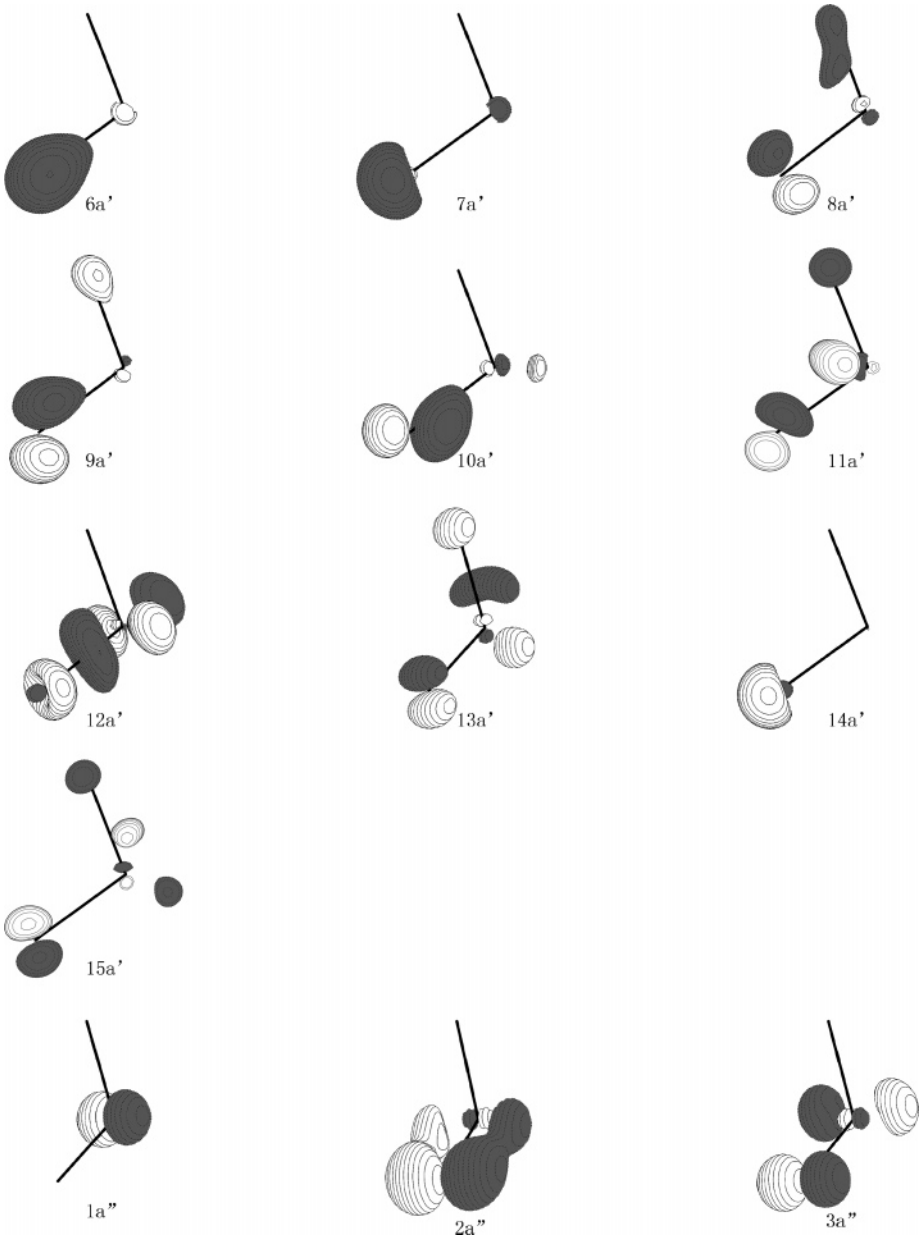

Figure 1. Plots of the electronic density of the orbital included in the active space used through the optimization process.

calculated $R_{(O-S)} = 1.704$ Å, $R_{(H-S)} = 1.339$ Å, and $\Phi_{(H-S-O)} = 95.0°$ in another CASSCF calculation.[8,14]

The $3^2A''$ state corresponds to an valence $\pi \rightarrow p^*$ transition and has a dominant configuration $(core)(6a')^2(7a')^2(8a')^2(9a')^2(2a'')^1(10a')^2(3a'')^2$ with a coefficient of -0.91, which is slightly modified by two other leading configurations with coefficients above 0.1 as shown in Table 2. This state can simply be regarded as a single-electron transition $2a'' \rightarrow 3a''$. The orbital $2a''$ is of π type bonding character and composed mainly of the $2p_z$ of the oxygen atom and $3p_z$ of the sulfur atom. The optimized geometries for this state are $R_{(H-S)} = 1.361$ Å, $R_{(O-S)} = 1.797$ Å, and $\Phi_{(H-S-O)} = 100.4°$. As compared to the ground state, $R_{(H-S)}$ is shortened to 0.04 Å, $R_{(O-S)}$ is elongated to 0.31 Å, and the bond angle is decreased to 4.4°, respectively.

We note the obvious elongation of $R_{(H-S)}$ appears for the $2^2A'$ state, in which the $R_{(H-S)}$ is elongated from 1.385 to 1.676 Å, $R_{(O-S)}$ is elongated to 0.045 Å, and the $\Phi_{(H-S-O)}$ expands to 3.0°. The excited state $2^2A'$ has the trend to bend and decompose to the SO fragment and the sulfur atom, which has been touched in a classical dynamic calculation.[22] State $2^2A'$ has a dominant leading configuration $(core)(6a')^2(7a')^2(8a')^2\ (9a')^2(2a'')^2(10a')^2(3a'')^0(11a')^1$ slightly modified by the other two configurations. The dominant leading configuration can also be described by a single-electron transition $3a'' \rightarrow 11a'$. The d component of the sulfur atom is important for the character assignment of the $11a'$ orbital, which is composed of varied levels of s, p_x, p_y, and d components of sulfur atom, p_x and p_y components of oxygen atom, and a small amount of immingled 1s of hydrogen. Because of the participation of the d component of the sulfur atom in the $11a'$ orbital, the bonding effect between sulfur and oxygen atoms is counteracted, and finally, this orbital exhibits antibonding character. This assignment for $11a'$ orbital is also supported by the SCF and CI calculation results.[14] For the single-electron transition $3a'' \rightarrow 11a'$, the repulsive interaction between hydrogen and sulfur atoms in orbital $11a'$ makes the S−H bond shortened to 0.294 Å. Because the interaction between sulfur and oxygen atoms in both orbitals are of antibonding character, the $R_{(O-S)}$ is just elongated to 0.044 Å after the transition. The bond angle expands from ground 104.8° to excited state's 107.8°, and this is easily explained by the repulsive interaction

TABLE 3: Vibration Frequencies for the Geometries of Ground and the Excited States Calculated in the ANO-L Basis Set at the CASSCF Level

	harmonic vibration frequency (cm^{-1})			experimental data (cm^{-1})		
state	v_1	v_2	v_3	v_1	v_2	v_3
X^2A''	2302.4 (74.1)	1108.7 (25.3)	1033.9 (12.6)	2447.90[a]	1101.59[a]	1027.4[a]
				2271[b]	1164[b]	1026[b]
				2570[c]	1063[c]	1013[c]
$1^2A'$	2550.4 (5.93)	872.1 (15.5)	731.5 (5.23)	2754[b]	852[b]	672[b]
				2769[c]	828[c]	702 ± 5[c]
				2769[d]	828[d]	702[d]
$2^2A'$	1056.1 (6.80)	891.4 (4.93)	707.7 (59.0)			
$3^2A''$	2433.7 (16.4)	834.8 (1.04)	600.1 (85.6)			

[a] Ref 16. [b] Ref 8. [c] Ref 5. [d] Ref 20.

TABLE 4: Vertical Ionization Energies of the HSO Neutral Radical Calculated Based on the Geometry of the Ground State of the Neutral Radical in the ANO-L Basis Set[a]

	vertical ionization energy (eV)		adiabatical ionization energy (eV)		
state	CASSCF	CASPT2	CASSCF	CASPT2	previous results (eV)
X^1A'	9.82	9.79	8.76	9.77	9.918 ± 0.016[b], 9.925[c], 9.897[d]
$1^3A''$	10.89	10.88	10.14	10.85	11.15 ± 0.04[b], 12.878[c], 11.204[d]
$2^1A''$	11.59	11.55	10.74	11.49	
$3^3A'$	13.46	13.35	11.83	12.69	
$4^3A''$	14.27	14.25	13.41	14.05	
$5^1A'$	14.97	14.69	13.79	14.54	
$6^1A''$	14.95	14.78			
$7^3A''$	15.87	15.80	14.65	15.05	
$8^3A'$	16.41	15.87	14.70	15.20	
$9^1A''$	16.26	16.08			
$10^3A'$	16.71	16.37			
$11^3A'$	18.36	17.29			
$12^3A'$	19.23	18.24			
$13^1A''$	18.91	18.37	16.33	16.71	
$14^3A'$	19.69	18.90			

[a] The relative energies are obtained and compared to the ground states energies -473.16187 au at the CASSCF level and -473.62117 au at the CASPT2 level. [b] Experimental results in ref 41. [c] Vertical ionization energies calculated at the G2 level in ref 41. [d] Adiabatic ionization energies calculated at the G2 level in ref 41.

TABLE 5: Structure Parameters, Harmonic Frequencies, and Relative Energies of the HSO^+ Cation in Both Levels Calculated Adiabatically by Using the ANO-L Basis Set[a]

	harmonic frequencies			structural parameters		
state	ω_1	ω_2	ω_3	R_{H-S}	R_{O-S}	Φ_{H-S-O}
X^1A'	2337.4	1238.1	1078.6	1.395	1.443	104.3
$1^3A''$	2292.6	972.8	734.4	1.388	1.524	96.2
$2^1A''$	2171.5	898.1	820.5	1.401	1.542	94.5
$3^3A'$	2441.7	979.4	747.1	1.375	1.696	98.6
$4^3A''$	2316.1	985.5	804.5	1.391	1.607	108.7
$5^1A'$	2312.4	944.6	329.5	1.389	1.549	128.5
$7^3A''$	1510.6	907.5	356.1	1.376	1.842	86.8
$8^3A'$	2356.8	698.2	611.5	1.382	1.739	116.0
$13^1A''$	3000.2	930.1	826.4	1.642	1.613	73.1

[a] The bond lengths are in units of Å, the bond angles are in units of °, and the frequencies are in units of cm^{-1}; all of the data are obtained at the CASSCF level in the ANO-L basis set.

between the two end atoms and the middle sulfur atom in orbital 11a′. To our best knowledge, there are not any geometrical data about states $2^2A'$ and $3^2A''$ in the literature.

After the geometry optimizations, the frequency analyses are also performed. In Table 3, we list the harmonic vibration frequency values corresponding to three types of normal modes, which are v_1 of a S−H bond-stretching mode, v_2 of a H−S−O bending vibration mode, and v_3 of a H−O bond-stretching mode. The frequencies of the ground state are determined as 2302.4, 1108.8, and 1033.9 cm^{-1} with intensity values of 74.1, 25.3, and 12.6 corresponding to v_1, v_2, and v_3, respectively. The v_1 value is obtained for the first time in theory. These ground data support the results from direct experimental measurement and a little deviated from 2271 cm^{-1}, which are deduced from the corresponding DSO fundamentals by multiplication with an appropriate isotope factor and the theoretical calculation.[8] All of the frequencies are real, and the optimized electronic states are confirmed to be stationary points in respective potential energy surfaces. The alteration of frequencies is also consistent with the change of the geometries and other available data shown in Table 3.

TABLE 6: Electronic Configurations of the Electronic States of the HSO^+ Cation Calculated Adiabatically at the CASSCF Level by Using the ANO-L Basis Set

		configuration											
state	coeff	6a′	7a′	8a′	9a′	2a″	10a′	3a″	11a′	12a′	13a′	14a′	15a′
X^1A'	0.94	2	2	2	2	2	2	0	0	0	0	0	0
	0.16	2	2	2	2	0	2	2	0	0	0	0	0
$1^3A''$	−0.95	2	2	2	2	2	1	1	0	0	0	0	0
$2^1A''$	−0.95	2	2	2	2	2	1	1	0	0	0	0	0
	−0.12	2	2	1	2	1	2	2	0	0	0	0	0
$3^3A'$	0.96	2	2	2	2	1	2	1	0	0	0	0	0
$4^3A''$	0.90	2	2	2	1	2	2	1	0	0	0	0	0
	0.31	2	2	2	2	1	1	2	0	0	0	0	0
$5^1A'$	0.91	2	2	2	2	2	0	2	0	0	0	0	0
	−0.28	2	2	2	0	2	2	2	0	0	0	0	0
$7^3A''$	−0.75	2	2	1	2	2	2	1	0	0	0	0	0
	0.54	2	2	2	2	1	1	2	0	0	0	0	0
	0.10	2	2	0	2	2	2	1	1	0	0	0	0
$8^3A'$	0.95	2	2	2	1	2	1	2	0	0	0	0	0
$13^1A''$	−0.61	2	2	2	2	2	1	1	0	0	0	0	0
	−0.41	2	2	2	1	2	2	1	0	0	0	0	0
	−0.39	2	2	2	0	2	2	1	1	0	0	0	0
	0.33	2	2	2	1	2	1	1	1	0	0	0	0
	−0.19	2	2	2	1	1	2	2	0	0	0	0	0
	0.15	2	2	0	2	2	2	1	1	0	0	0	0
	−0.15	2	2	1	1	2	2	1	1	0	0	0	0

Equilibrium Geometries of the HSO^+ Cation. A total of nine ionic states of HSO^+ cation are optimized adiabatically, and the frequency analyses are also performed. The structural parameters and harmonic frequencies can be found in Table 5, and the configuration information can be found in Table 6.

On the basis of adiabatic energies, the $1^1A'$ state is confirmed as the ground state of HSO^+ cation, which has a dominant leading configuration $(core)(6a')^2(7a')^2(8a')^2(9a')^2\ (2a'')^2(10a')^2(3a'')^0$ with a coefficient of 0.94 slightly modified by a double promotion $2a'' \rightarrow 3a''$ with a coefficient of 0.16. As compared to the neutral radical's electronic structure, this state can result from eliminating the single electron in the 3a″ orbital (π^* type) of the ground neutral radical. This electron's elimination makes the $R_{(O-S)}$ shortened to 0.050 Å, but other geometry parameters are almost unchanged. The final structural parameters of the

$1^1A'$ state are $R_{(O-S)} = 1.443$ Å, $R_{(H-S)} = 1.395$ Å, and $\Phi_{(H-S-O)} = 104.3°$, consistent with the $R_{(O-S)} = 1.493$ Å, $R_{(H-S)} = 1.389$ Å, and $\Phi_{(H-S-O)} = 103.87°$ calculated at the MP4-FC level and the UHF level.[31]

The single-electron transition $10a' \rightarrow 3a''$ in parallel spin results in the first ionic excited state $1^3A''$, which has only one leading configuration (core)$(6a')^2(7a')^2(8a')^2\,(9a')^2(2a'')^2(10a')^1(3a'')^1$ with a coefficient of 0.95. The calculated geometrical parameters are $R_{(O-S)} = 1.524$ Å, $R_{(H-S)} = 1.388$ Å, and $\Phi_{(H-S-O)} = 96.2°$, which agree with the calculated values $R_{(O-S)} = 1.584$ Å, $R_{(H-S)} = 1.380$ Å, and $\Phi_{(H-S-O)} = 92.8°$, respectively.[31] This state is located at 1.08 eV at the CASPT2/ANO-L level and 1.38 eV at the CASSCF/ANO-L level above the $1^1A'$ ground ionic state. This is consistent with the theoretical result performed by Buenker et al.[16] but obviously conflicts with the HF results from the ref 31, in which the $1^3A''$ state was located at 0.9 kcal/mol lower than the $1^1A'$ state and was assigned as the ground state of the HSO^+ cation. Considering the antibonding character of the 3a″ orbital,[15,20] our results are more reasonable.

Obviously, transition $10a' \rightarrow 3a''$ in unparallel spin needs a little more energy and can result in the lowest cationic $2^1A''$ state, which is composed of the configuration (core)$(6a')^2(7a')^2(8a')^2(9a')^2(2a'')^2(10a')^1(3a'')^1$ with a coefficient of 0.95 accompanied by the configuration (core)$(6a')^2(7a')^2(8a')^1(9a')^2(2a'')^1(10a')^2(3a'')^2$ with a coefficient of 0.12. The 8a′ orbital is mainly of antibonding character resulting from the interaction of the p_{xy} hybridized orbital between the oxygen and the sulfur atoms with a strong attracted interaction between the hydrogen and the oxygen atoms. Another three orbitals have been designed in the last section. So, as compared to the ground HSO^+ cation, the $R_{(O-S)}$ is elongated to 0.099 Å and the $\Phi_{(H-S-O)}$ shrinks to 8.1° after the promotion. The final geometrical parameters calculated in this paper are $R_{(O-S)} = 1.542$ Å, $R_{(H-S)} = 1.401$ Å, and $\Phi_{(H-S-O)} = 94.5°$, respectively.

The third electron excited state of the cation is the $3^3A'$ state, which has a dominant leading configuration (core)$(6a')^2(7a')^2(8a')^1(9a')^2(2a'')^1(10a')^2(3a'')^1$ corresponding to the single-electron transition $2a'' \rightarrow 3a''$ ($\pi \rightarrow p^*$). Therefore, the $R_{(O-S)}$ is elongated to about 0.253 Å as compared to the ground value. Total geometrical parameters of the $3^3A'$ state are $R_{(H-S)} = 1.375$ Å, $R_{(O-S)} = 1.696$ Å, and $\Phi_{(H-S-O)} = 98.6°$.

For the third lowest triplet electronic state $4^3A''$, the $\Phi_{(H-S-O)}$ is 108.6°, close to the ground cation. In state $4^3A''$, the multielectron transitions hold important positions because this state has two dominant leading configurations (core)$(6a')^2(7a')^2(8a')^2(9a')^1(2a'')^2(10a')^2(3a'')^1$ with the coefficient of 0.90 and (core)$(6a')^2(7a')^2\,(8a')^2(9a')^2(2a'')^1(10a')^1(3a'')^2$ with the coefficient of 0.31, for which the former can be described with a single-electron transition $9a' \rightarrow 3a''$ and the latter is a multielectron transition configuration. From Figure 1, we can find that the 9a′ orbital is of nonbonding character composed mainly of p_y components of the oxygen and sulfur atoms, the s component of the hydrogen atom. So, after the electron promotion to the 3a″ (π^*) orbital, the angle is increased to 4.4°, and the $R_{(O-S)}$ is elongated to 0.164 Å. The final geometrical data are $R_{(H-S)} = 1.391$ Å, $R_{(O-S)} = 1.607$ Å, and $\Phi_{(H-S-O)} = 108.7°$.

The largest angle appears in the $5^1A'$ state, in which the angle is increased from 104.3° of the ground cation to 128.5° of the excited state. This state has two distinct double transition configurations $10a' \rightarrow 3a''$ and $9a' \rightarrow 3a''$ with the coefficients 0.91 and −0.28, respectively. The transition $10a' \rightarrow 3a''$ makes the angle of the excited state showing severe expansion. The final optimized geometrical data are $R_{(H-S)} = 1.389$ Å, $R_{(O-S)} = 1.549$ Å, and $\Phi_{(H-S-O)} = 128.5°$.

TABLE 7: Vertical Excited Energy of HSO Neutral Radical Calculated in CASSCF and CASPT2 Methods by Using the ANO-L$^+$ Basis Set[a]

		eV		
state	nature	CASSCF	CASPT2	*f*
X^2A''		0.00	0.00	ground state
$1^2A'$		3.78	2.50	0.00025
$2^2A'$		5.08	4.46	0.00045
$4^2A'$		6.57	5.46	0.00254
$7^2A'$		7.29	6.16	0.00015
$8^2A'$ (Rydberg)	$3a'' \rightarrow 3s$	7.87	6.84	0.03518
$10^2A'$ (Rydberg)	$3a'' \rightarrow 3p_y$	8.17	7.59	0.00127
$12^2A'$ (Rydberg)	$3a'' \rightarrow 3p_x$	8.93	8.10	0.01096
X^2A''		0.00	0.00	ground state
$3^2A''$		5.89	4.66	0.06263
$5^2A''$		7.01	6.02	0.00100
$6^2A''$		7.55	6.14	0.02774
$9^2A''$ (Rydberg)	$3a'' \rightarrow 3p_z$	8.12	7.35	0.09393
$11^2A''$ (Rydberg)	$3a'' \rightarrow 3d_{yz}$	8.39	7.99	0.03425
$13^2A''$ (Rydberg)	$3a'' \rightarrow 3d_{xz}$	9.64	8.75	0.07001
$14^2A''$ (Rydberg)	$3a'' \rightarrow 4p_z$	10.78	9.95	0.01761
$15^2A''$ (Rydberg)	$3a'' \rightarrow 5p_z$	11.46	10.35	0.00106

[a] For the different symmetries, we have chosen different active spaces. The relative energies are obtained from the comparison between the excited states' energy and the ground energy calculated in the same active space. All of the energies are shifted 0.1 au with the imaginary shift technology. All of the weight values of zero-order wave function in the first-order wave functions are above 90%.

The $R_{(O-S)}$ is elongated most severely for state $7^3A''$, in which it is elongated 0.399 Å. This state can be described by three electronic configurations as shown in Table 6. The second two configurations are multielectron transition configurations with the coefficients 0.54 and 0.10, respectively. The total geometrical parameters are $R_{(H-S)} = 1.376$ Å, $R_{(O-S)} = 1.842$ Å, and $\Phi_{(H-S-O)} = 86.8°$.

Another state $8^3A'$ with largely elongated $R_{(O-S)}$ does not show angle shrinkage. This state has only one dominant leading configuration (core)$(6a')^2(7a')^2(8a')^2(9a')^1\,(2a'')^2(10a')^1(3a'')^1$, which is a multielectron excitation configuration, and the total geometrical parameters are $R_{(H-S)} = 1.382$ Å, $R_{(O-S)} = 1.739$ Å, and $\Phi_{(H-S-O)} = 116.0°$. The most apparent multiconfiguration effect appears in the $13^1A''$ state, which has a total of seven leading configurations with the coefficients above 0.1. The geometrical parameters and the detailed configurations are listed in Tables 5 and 6.

The calculated harmonic frequencies for ionic states are collected in Table 5. Through the harmonic frequency analyses, all of the geometries are confirmed as the stationary points in the potential energy surfaces.

Ionization Energy of the HSO Neutral Radical. The accurate theoretical prediction of electron ionization energy is traditionally one of the most demanding fields in quantum chemical calculations. Adiabatic ionization potentials of HSO neutral radical can been obtained by using the equilibrium total energies of the neutral and cationic species. The vertical ionization potentials can be obtained based on the equilibrium geometry of the ground neutral radical. The final data are listed in Table 4.

The first ionization energy is confirmed as 9.77 eV at the CASPT2 level adiabatically. In the vertical ionization calculations, the similar ionization energy 9.79 eV is obtained at the CASPT2 level, and the energy separation between them is 0.02 eV. A similar case happens for the two other higher states $1^3A''$ and $2^1A''$, which have adiabatic ionization energies of 10.85

TABLE 8: Configurations Obtained from the Vertical Calculations Performed at the CASPT2 Level for $^2A''$ Symmetry by Using the ANO-L$^+$ Basis Set

		configuration													
state	coeff	10a′	11a′	2a″	3a″	4a″	5a″	6a″	7a″	8a″	9a″	10a″	11a″	12a″	13a″
X^2A''	0.98	2	0	2	1	0	0	0	0	0	0	0	0	0	0
	−0.11	2	0	2	0	0	0	0	0	0	0	1	0	0	0
$3^2A''$	−0.97	2	0	1	2	0	0	0	0	0	0	0	0	0	0
	0.15	2	0	2	0	0	0	0	0	0	0	1	0	0	0
	0.13	2	0	1	1	0	0	0	0	0	0	0	0	0	0
	0.11	2	0	1	1	0	0	0	0	0	0	1	0	0	0
$5^2A''$	0.85	2	0	2	1	0	0	0	0	0	0	0	0	0	0
	0.43	1	1	2	1	0	0	0	0	0	0	0	0	0	0
	0.22	1	1	1	2	0	0	0	0	0	0	0	0	0	0
$6^2A''$	0.88	2	0	2	1	0	0	0	0	0	0	0	0	0	0
	−0.35	1	1	2	1	0	0	0	0	0	0	0	0	0	0
	0.28	1	1	1	2	0	0	0	0	0	0	0	0	0	0
	−0.15	1	1	1	2	0	0	0	0	0	0	0	0	0	0
$9^2A''$ (Rydberg)	0.91	2	0	2	0	1	0	0	0	0	0	0	0	0	0
	−0.25	2	0	0	2	1	0	0	0	0	0	0	0	0	0
	−0.16	2	0	2	0	0	0	1	0	0	0	0	0	0	0
	−0.14-	2	0	2	0	0	1	0	0	0	0	0	0	0	0
	−0.10	2	0	1	1	1	0	0	0	0	0	0	0	0	0
	−0.10	1	1	2	1	0	0	0	0	0	0	0	0	0	0
$11^2A''$ (Rydberg)	0.93	2	0	2	0	0	1	0	0	0	0	0	0	0	0
	−0.26	2	0	0	2	0	1	0	0	0	0	0	0	0	0
	0.15	2	0	2	0	1	0	0	0	0	0	0	0	0	0
$13^2A''$ (Rydberg)	0.88	2	0	2	0	0	0	1	0	0	0	0	0	0	0
	0.33	2	0	2	0	0	0	0	1	0	0	0	0	0	0
	−0.24	2	0	0	2	0	0	2	0	0	0	0	0	0	0
	0.11	2	0	2	0	1	0	0	0	0	0	0	0	0	0
	−0.10	2	0	1	1	0	0	1	0	0	0	0	0	0	0
$14^2A''$ (Rydberg)	0.86	2	0	2	0	0	0	0	1	0	0	0	0	0	0
	−0.32	2	0	2	0	0	0	1	0	0	0	0	0	0	0
	−0.24	2	0	0	2	0	0	0	1	0	0	0	0	0	0
	−0.17	2	0	2	0	0	0	0	0	0	1	0	0	0	0
	−0.14	2	0	2	0	1	0	0	0	0	0	0	0	0	0
	−0.11	2	0	1	1	0	0	0	1	0	0	0	0	0	0
$15^2A''$ (Rydberg)	−0.87-	2	0	2	0	0	0	0	0	0	1	0	0	0	0
	−0.28	2	0	1	1	0	1	0	0	0	0	0	0	0	0
	0.25	2	0	0	2	0	0	0	0	0	1	0	0	0	0
	−0.17	2	0	2	0	0	0	0	1	0	0	0	0	0	0
	0.10	2	0	1	1	1	0	0	0	0	0	0	0	0	0

and 11.49 eV and vertical ionization energies of 10.88 and 11.55 eV, respectively. The energy separation between the vertical and the adiabatic results is 0.03 eV for state $1^3A''$ and 0.06 eV for state $2^1A''$. So, we think that three fine structural lines can be expected corresponding to the lowest three ionic states of the HSO neutral radical in the photoelectron spectrum. The lowest two lines have been reported in the photoelectron spectrum,[41] but the third line has not yet been reported.

Ionic state $7^3A''$ has the adiabatic ionization energy 15.05 eV, which is 0.15 eV lower than the adiabatic ionization energies 15.20 eV of state $8^3A'$. This energy separation is lower than the frequency of the H−S stretching mode ($\omega_1 = 1510.6$ cm^{-1}) of the HSO^+ cation. So, the related two peaks would overlap each other in the photoelectron spectrum. Except for the lowest three ionic states, we think the other ionic states should be assigned to several bands in the photoelectron spectrum for the large energy separation between the vertical and the adiabatic results.

The ionization energy comparison among the HSS, HOO, and HSO molecules is also performed in Table 10. The oxygen atom is a second row element, and the sulfur atom is a third row element. So, the ionization energy of the sulfur is smaller than oxygen. Our calculated first ionization energy of the HSO molecule is located between the HOO and the HSS and the final ionization energy order is HOO > HSO > HSS.

Valence and Rydberg States of the HSO Neutral Radical. A total of 16 excited electronic states of the HSO neutral radical, seven for $^2A'$ symmetry and nine for $^2A''$ symmetry, are explored vertically with both CASSCF and CASPT2 methods by using the ANO-L$^+$ basis set, and the final data are listed in Table 7. The leading configurations of the respective states at CASPT2 level are listed in Table 8 for $^2A''$ symmetry and in Table 9 for $^2A'$ symmetry. All of the vertical calculations are performed based on the equilibrium geometry of the neutral ground state. For the purpose of comparison, the adiabatic excited energies are also calculated at the same theoretical level using the ANO-L basis set for the lowest four electronic states, and the final data are listed in Table 1.

Electronic excited states may be of valence or Rydberg character. In the vertical calculations, the character of the excited states can be easily confirmed from the state's dominant leading configurations and the expectation value of the operator $\langle z^2 \rangle$, which should be markedly larger for the Rydberg states than the valence states. In our calculations, eight valence excited states are estimated finally as X^2A'', $1^2A'$, $2^2A'$, $3^2A''$, $4^2A'$, $5^2A''$, $7^2A'$, and $6^2A''$ in an increasing energy order and others are of Rydberg character.

The lowest four electronic states are probed in both the vertical and the adiabatic calculations. Although they are in the same energy order from two types of calculations, the leading configurations for these electronic states do not always keep the same states vertically and adiabatically. Ground-state X^2A'' has only one leading configuration with a coefficient adiabatically above 0.1, but in the vertical calculation results, another

TABLE 9: Configurations Obtained from the Vertical Calculations Performed at the CASPT2 Level for $^2A'$ Symmetry by Using the ANO-L$^+$ Basis Set

		configuration														
state	coeff	9a′	10a′	11a′	12a′	13a′	14a′	15a′	16a′	17a′	18a′	19a′	20a′	2a″	3a″	4a″
$1^2A'$	0.96	2	1	0	0	0	0	0	0	0	0	0	0	2	2	0
	−0.19	1	2	0	0	0	0	0	0	0	0	0	0	2	2	0
$2^2A'$	−0.24	2	2	1	0	0	0	0	0	0	0	0	0	2	0	0
	−0.15	2	2	0	1	0	0	0	0	0	0	0	0	2	0	0
	0.44	2	2	0	0	0	1	0	0	0	0	0	0	2	0	0
	−0.78	2	2	0	0	0	0	1	0	0	0	0	0	2	0	0
	0.17	2	2	0	0	0	0	1	0	0	0	0	0	0	2	0
$4^2A'$	0.44	2	2	1	0	0	0	0	0	0	0	0	0	2	0	0
	−0.21	2	2	0	1	0	0	0	0	0	0	0	0	2	0	0
	−0.66	2	2	0	0	0	1	0	0	0	0	0	0	2	0	0
	0.14	2	2	0	0	0	1	0	0	0	0	0	0	0	2	0
	−0.45	2	2	0	0	0	0	1	0	0	0	0	0	2	0	0
	0.11	2	2	0	0	0	0	1	0	0	0	0	0	0	2	0
	0.11	1	2	0	0	0	0	0	0	0	0	0	0	2	2	0
$7^2A'$	−0.12	2	2	1	0	0	0	0	0	0	0	0	0	2	0	0
	0.19	2	1	0	0	0	0	0	0	0	0	0	0	2	2	0
	0.94	1	2	0	0	0	0	0	0	0	0	0	0	2	2	0
$8^2A'$ (Rydberg)	0.67	2	2	1	0	0	0	0	0	0	0	0	0	2	0	0
	−0.15	2	2	1	0	0	0	0	0	0	0	0	0	0	2	0
	−0.38	2	2	0	1	0	0	0	0	0	0	0	0	2	0	0
	−0.21	2	2	0	0	1	0	0	0	0	0	0	0	2	0	0
	0.46	2	2	0	0	0	1	0	0	0	0	0	0	2	0	0
	0.12	2	2	0	0	0	0	1	0	0	0	0	0	2	0	0
$10^2A'$ (Rydberg)	0.22	2	2	0	1	0	0	0	0	0	0	0	0	2	0	0
	−0.91	2	2	0	0	1	0	0	0	0	0	0	0	2	0	0
	0.20	2	2	0	0	1	0	0	0	0	0	0	0	0	2	0
	−0.14	2	2	0	0	0	1	0	0	0	0	0	0	2	0	0
$12^2A'$ (Rydberg)	0.42	2	2	1	0	0	0	0	0	0	0	0	0	2	0	0
	−0.10	2	2	1	0	0	0	0	0	0	0	0	0	0	2	0
	0.78	2	2	0	1	0	0	0	0	0	0	0	0	2	0	0
	−0.17	2	2	0	1	0	0	0	0	0	0	0	0	0	2	0
	0.16	2	2	0	0	1	0	0	0	0	0	0	0	2	0	0
	0.18	2	2	0	0	0	1	0	0	0	0	0	0	2	0	0
	−0.18	2	2	0	0	0	0	1	0	0	0	0	0	2	0	0

TABLE 10: Ionization Energies of HSS, HOO, and HSO Radicals

species	theor (eV)	exp (eV)	ref
HSS	9.28		42
HSO	9.77		this work
		9.918 ± 0.016	13
HOO		11.35 ± 0.01	43
		11.67 ± 0.15	44
		11.53 ± 0.02	45
		11.54	46

configuration with a coefficient of −0.11 appears. This phenomena is more remarkable for electronic state $3^2A''$, for which the leading configurations are all different except the dominant. The $1^2A'$ electronic state, comprised of one dominant leading configuration with a coefficient about 0.96 adiabatically, has two configurations with the coefficient above 0.1 vertically. For the excited $2^2A'$ state, the leading configurations number is increased from adiabatic three to vertical four. It is clearly shown that we can get the same dominant leading configurations from the vertical and adiabatic calculations but the second configurations are a little different. At the CASPT2/ANO-L$^+$ level, we vertically locate the first excited state at 2.50 eV as compared to the adiabatic result of 1.84 eV above the ground state, which is consistent with the experimental value 1.29−2.38 eV determined through a chemiluminescence spectrum,[5] the spectral data 1.78 and 1.81 eV determined by a pulsed dye laser, the theoretical result of 1.81 eV using the CASSCF+1+2 method in the cc-pVQZ basis set, and better than the theoretical results of 1.48 and 1.71 eV listed in Table 1.[32,20] The lowest three excited states at 1.84, 3.92, and 3.98 eV adiabatically at the CASPT2 level are located at 2.50, 4.46, and 4.66 eV vertically related to ground-state X^2A''. A marked deviation between the adiabatic and the vertical excited energies makes us predict the severe geometrical deviation of the excited states' equilibrium geometries as compared to the ground state, just as shown in the geometry optimization section. Besides the valence states mentioned above, another three higher valence states also have been touched in the vertical calculations. They are states $4^2A'$, $5^2A''$, and $6^2A''$ lying at 5.46, 6.02, and 6.14 eV relative to neutral ground-state X^2A'', respectively. State $4^2A'$ has a complex configuration structure, which is composed mainly of three single transitions 3a″ → 11a′, 3a″ → 14a′, and 3a″ → 15a′ configurations with the coefficients of 0.44, −0.66, and −0.45, respectively. The $5^2A''$ and $6^2A''$ states have several dominant leading configurations corresponding to complex transitions happening in orbitals 2a″, 10a′, 11a′, and 3a″. The highest valence excited state confirmed by us is $7^2A'$, which can be regarded as an inner shell single-electron transition 9a′ → 3a″.

At the CASPT2/ANO-L$^+$ level, a total eight Rydberg states are confirmed in an energy range of 6.84−10.35 eV from this paper. These Rydberg states all correspond to the transitions from the HOMO (3a″) to the Rydberg orbital. Through the analyses of the orbital component and the charge population, these eight Rydberg states ($8^2A'$, $9^2A''$, $10^2A'$, $11^2A''$, $12^2A'$, $13^2A''$, $14^2A''$, and $15^2A''$) are assigned to the transitions 3a″ → 3s, $3p_z$, $3p_y$, $3d_{yz}$, $3p_x$, $3d_{xz}$, $4p_z$, and $5p_z$ Rydberg orbital and are located at 6.84, 7.35, 7.59, 7.99, 8.10, 8.75, 9.95, and 10.35 eV relative to neutral ground-state X^2A'', respectively. To our best knowledge, this paper reports the Rydberg states of the HSO neutral radical for the first time.

From the CASSCF and CASPT2 methods adopted in this paper, we obtain the zero-order wave function through the CASSCF calculation and mix them up to constitute the configurations space used in the CASPT2 calculations. We can not only obtain more accurate energy values through the CASPT2 calculations but also separate the configurations mixture effectively. This can be found from the components variation between the adopted two methods. For instance, state $3^2A''$ has two dominant leading configurations corresponding to the single-electron transitions $2a'' \rightarrow 3a''$ and $10a' \rightarrow 11a'$ with coefficients of -0.81 and 0.47 at CASSCF, respectively. However, at the CASPT2 level, the coefficient of the transition $2a'' \rightarrow 3a''$ is increased to -0.95 and the other dominant configuration disappears from the leading configurations list. Even though the states without severe configuration mixtures, the CASPT2 method can also strengthen the status of the dominant leading configuration and make the electronic state show a clearer transition nature.

Considering the important meaning of the ab initio calculations in simulating the chemiluminescence precisely, we calculate the oscillator strength values corresponding to the vertical transition from the excited states to the neutral ground-state X^2A'', and these data are listed in the last row of Table 7. Eight states with the oscillator strength above 0.01 have been found.

Conclusion

Four electronic states of HSO neutral radical and nine ionic states of HSO^+ cation are optimized, and the detailed electron configurations and geometrical data are obtained adiabatically at the CASSCF level by using the ANO-L basis set. The electronic configurations are used to explain the geometrical alteration in detail. The vertical ionization energy in a wide range of 9.79−18.90 eV is assigned to a total of 15 ionic states at the CASPT2 level. The lowest three ionization energies are also confirmed as 9.77, 10.85, and 11.49 eV at the CASPT2 level adiabatically. Through the comparison between the vertical and the adiabatic ionization energies, three sharp peaks are expected in the photoelectron spectrum, which is consistent with the experimental results.[41] Furthermore, through the vertical transition calculations of the neutral radical, a total of 16 electronic states (including eight Rydberg states) are located below 10.35 eV relative to the neutral ground state. We assign these eight Rydberg states ($8^2A'$, $9^2A''$, $10^2A'$, $11^2A''$, $12^2A'$, $13^2A''$, $14^2A''$, and $15^2A''$) to the transition $3a'' \rightarrow 3s$, $3p_z$, $3p_y$, $3d_{yz}$, $3p_x$, $3d_{xz}$, $4p_z$, and $5p_z$ Rydberg orbital, respectively, and locate them at 6.84, 7.35, 7.59, 7.99, 8.10, 8.75, 9.95, and 10.35 eV relative to neutral ground-state X^2A''. From the comparison between the CASSCF and the CASPT2 methods, we confirm that the CASPT2 method can separate the configurations mixture effectively.

Acknowledgment. This work is supported by the National Science Foundation of China nos. 20573042, 20173021, and 20333050.

References and Notes

(1) Kendall, D. J. W.; O'Brien, J. J. A.; Sloan, J. J. *Chem. Phys. Lett.* **1984**, *110*, 183.
(2) Wang, N. S.; Lovejoy, E. R.; Howad, C. J. *J. Phys. Chem.* **1987**, *91*, 5743.
(3) Lovejoy, E. R.; Wang, N. S.; Howard, C. J. *J. Phys. Chem.* **1987**, *91*, 5749.
(4) Wang, N. S.; Howard, C. J. *J. Phys. Chem.* **1990**, *94*, 8787.
(5) Schurath, U.; Weber, M.; Becker, K. H. *J. Chem. Phys.* **1977**, *67*, 110.
(6) Slagle, I. R.; Baiocchi, F.; Gutman, D. *J. Phys. Chem.* **1978**, *82*, 1333.
(7) Kakimoto, M.; Saito, S.; Hirota, E. *J. Mol. Spectrosc.* **1980**, *80*, 334.
(8) Ohashi, N.; Kakimoto, M.; Saito, S.; Hirota, E. *J. Mol. Spectrosc.* **1980**, *84*, 204.
(9) Davidson, F. E.; Clemo, A. R.; Duncan, D. L.; Browett, R. J.; Hobson, J. H.; Grice, R. *Mol. Phys.* **1985**, *46*, 33.
(10) Balucani, N.; Casavecchia, P.; Stranges, D.; Volgi, G. G. *Chem. Phys. Lett.* **1993**, *211*, 469.
(11) Iraqi, M.; Goldberg, N.; Schwarz, H. *J. Phys. Chem.* **1994**, *98*, 2015.
(12) (a) Balucani, N.; Stranges, D.; Casavecchia, P.; Volpi, G. G. *J. Chem. Phys.* **2004**, *120*, 9571. (b) Quandt, R. W.; Wang, X.; Tsukiyama, K.; Bersohn, R. *Chem. Phys. Lett.* **1997**, *276*, 122.
(13) Sannigrahi, A. B.; Thunemann, K. H.; Peyerimhoff, S. D.; Buenker, R. J. *Chem. Phys.* **1977**, *20*, 25.
(14) Sannigrahi, A. B.; Peyerimhoff, S. D.; Buenker, R. J. *Chem. Phys.* **1977**, *20*, 381.
(15) Luke, B. T.; McLean, A. D. *J. Phys. Chem.* **1985**, *89*, 4592.
(16) Buenker, R. J.; Bruna, P. J.; Peyerimhoff, S. D. *Isr. J. Chem.* **1980**, *19*, 309.
(17) Tyndall, G. S.; Ravishankara, A. R. *Int. J. Chem. Kinet.* **1991**, *23*, 483.
(18) Kendall, R. A.; Dunning, T. H., Jr.; Harrison, R. J. *J. Chem. Phys.* **1992**, *96*, 6796.
(19) Xantheas, S. S.; Dunning, T. H., Jr. *J. Phys. Chem.* **1993**, *97*, 18.
(20) Xantheas, S. S.; Dunning, T. H., Jr. *J. Phys. Chem.* **1993**, *97*, 6616.
(21) Martínez-Núñez, E.; Varandas, A. J. C. *J. Phys. Chem. A* **2001**, *105*, 5923.
(22) Martinez-Núñez, E.; Vázquez, S. A.; Varandas, A. J. C. *Phys. Chem. Chem. Phys.* **2002**, *4*, 279.
(23) Espinosa-Garcia, J.; Corchado, J. C. *Chem. Phys. Lett.* **1994**, *218*, 128.
(24) Esseffar, M.; Mó, O.; Yáñez, M. *J. Chem. Phys.* **1994**, *101*, 2175.
(25) Wilson, C.; Hirst, M. D. *J. Chem. Soc., Faraday. Trans.* **1994**, *90*, 3051.
(26) Goumri, A.; Laakso, D.; Smith, C. E.; Rocha, J.-D.; Marshall, P. *J. Chem. Phys.* **1995**, *102*, 161.
(27) Denis, P. A.; Ventura, O. N. *Int. J. Quantum Chem.* **2000**, *80*, 439.
(28) Badenes, M. P.; Tucceri, M. E.; Cobos, C. J. *Z. Phys. Chem.* **2000**, *214*, 1193.
(29) Wilson, A. K.; Dunning, T. H. *J. Phys. Chem. A* **2004**, *108*, 3129.
(30) Denis, P. A. *Chem. Phys. Lett.* **2005**, *402*, 289.
(31) Moore Plummer, P. L. *J. Chem. Phys.* **1990**, *92*, 6627.
(32) Kawasaki, M.; Tanahashi, S.; Tanahashi, K.; Sato, H. *J. Chem. Phys.* **1983**, *78*, 7146.
(33) Kawasaki, M.; Kasatani, K.; Sato, H. *Chem. Phys. Lett.* **1980**, *75*, 128.
(34) Kendall, D. J. W.; O'Brien, J. J. A.; Sloan, J. J. *Chem. Phys. Lett.* **1984**, *110*, 183.
(35) Roos, B. O. In *Advance in Chemical Physica; Ab Initio Methods in Quantum Chemistry—II*; Lawley, K. P., Ed.; John Wiley & Sons Ltd.: Chichester, England, 1987; p 399.
(36) Pierloot, K.; Dumez, B.; Widmark, P.-O.; Roos, B. O. *Theor. Chim. Acta* **1995**, *90*, 87.
(37) Andersson, K.; Malmqvist, P.-A.; Roos, B. O. *J. Chem. Phys.* **1992**, *96*, 1218.
(38) Andersson, K.; Roos, B. O. Modern electron structure theory. In *Advanced Series in Physical Chemistry*; Yarkony, R., Ed.; Word Scientific Publishing Co. Pte. Ltd.: Singapore, 1995; Vol. 2, Part I, p 55.
(39) Kaufmann, K.; Baumeister, W.; Jungen, M. *J. Phys. B: At. Mol. Opt. Phys.* **1989**, *22*, 2223.
(40) Anderrson, K.; Bernhardsson, A.; Blomberg, M. R. A.; Boussard, P.; Cooper, D. L.; Fleig, T.; Fûlscher, M. P.; Karlstöm, G.; Lindh, R.; Malmqvist, P.-A.; Neogrády, P.; Olsen, J.; Roos, B. O.; Sadlej, A. J.; Schimmelpfennig, B.; Schûtz, M.; Seijo, L.; Serrano-Andrés, L.; Siegbahn, P. E. M.; Stålring, J.; Thorsteinsson, T.; Veryazov, V.; Wahlgren, U.; Widmark, P.-O. *MOLCAS Version 5.4*; Department of Theoretical Chemistry, Chemical Center, University of Lund: Lund, Sweden, 2000.
(41) Cheng, B. M.; Jürg, E.; Chen, W. C.; Yu, C. H. *J. Chem. Phys.* **1997**, *106* (23), 9727.
(42) Denis, P. A. *Chem. Phys. Lett.* **2006**, *422*, 434.
(43) Dyke, J. M.; Jonathan, N. B. H.; Morris, A.; Winter, M. *Mol. Phys.* **1981**, *44*, 1059.
(44) Tal'roze, V. L.; Butkovskaya, N. I.; Larichev, M. N.; Leipunskii, I. O.; Morozov, I. I.; Dodonov, A. F.; Kudrov, B. V.; Zelenov, V. V.; Raznikov, V. V. *Adv. Mass Spectrom.* **1978**, *7*, 693.
(45) Foner, S. N.; Hudson, R. L. *J. Chem. Phys.* **1955**, *23*, 1364.
(46) Dyke, J. M.; Jonathan, N. B. H.; Morris, A.; Winter, M. *Mol. Phys.* **1981**, *44*, 1059.